Journal of Energy Chemistry 63 (2021) 574–584

Contents lists available at ScienceDirect

Journal of Energy Chemistry

journal homepage: www.elsevier.com/locate/jechem

http://www.journals.elsevier.com/journal-of-energy-chemistry/

Liquid-like adsorbent assembled by CNTs: Serving as renewable CO_2 capture materials for indoor air

Jae Won Lee, Minjae Kim, Han Sol Jung, Ronghuan Xu, Seonggon Kim, Yong Tae Kang *

School of Mechanical Engineering, Korea University, Seoul 02841, South Korea

ARTICLE INFO

Article history:
Received 3 May 2021
Revised 20 July 2021
Accepted 11 August 2021
Available online 20 August 2021

Keywords:
CO_2 capture
CNT
Silicone oil
Adsorbents
Indoor air

ABSTRACT

In this study, a CO_2 capture material in the form of liquid-like adsorbents (LLAs) is developed to overcome the limitations of conventional types of adsorbents. The increase in indoor activities necessitates the capture of CO_2 in enclosed indoor spaces. Indoor spaces require safe and stable materials for CO_2 capture because humans are present in these spaces. Solid adsorbents are mainly used because liquid absorbents are unsuitable owing to noise and scattering problems. In LLA, the liquid absorbent assembled by carbon nanotubes (CNTs) is solidified and prevented from flowing and scattering indoor. LLAs present to maintain 95% of initial capacity after recycling 20 times, and have characteristics that can be regenerated in a low temperature heat source (80 to 120 ℃) and moisture resistance. This work not only provides indoor useable CO_2 capture materials, but also offers a new prospect in the field of adsorbents.

1. Introduction

The demand for indoor air quality has increased along with the standard of living. Heating, ventilation, and air conditioning (HVAC) systems and household air purifiers that can effectively control the indoor air quality are increasingly being used. Air purifiers for home use are typically fine dust collectors based on high-efficiency particulate air (HEPA)-class fiber filters. In some cases, activated carbon filters are used to reduce the CO_2 level. However, there is no common standard for indoor CO_2 capture by air purifiers. Human indoor activities have increased in recent years because of the rising levels of dangerous substances such as fine dust, viruses, and bacteria in outdoors atmospheric environments. In an enclosed area, the CO_2 concentration can reach up to 5000 ppm [1], which is harmful to the human body. Therefore, direct air capture (DAC) technology has been recently studied as a method to remove CO_2 from low-concentration and humid air such as the atmosphere or indoors [2].

The most effective way to reduce indoor CO_2 is through ventilation. However, ventilation cannot be applied everywhere. DAC technology can be applied because indoor air conditions are similar to atmospheric conditions, but there are more considerations due to the specificity of human existence. Noise from fans in ventilation equipment or outside creates disturbances to quiet indoor activities. In subway trains, the concentration of CO_2 increases during rush hours because of the high people density. However, ventilation in subway trains is impossible because of the poor air quality in underground tunnels [3–5]. Various methods of removing CO_2, such as absorption, adsorption, and membrane [6], are used in industry. In absorption methods, the flow of absorbent produces noise when the absorbent drips. As the absorbent collides with the air stream, it can disperse into the air in the room. Amine-based solutions, which are representative absorbents, have unpleasant odor and create rust [7]. The adsorbent captures gas through microscopic pores over a large surface area. The adsorption capacity may be degraded when contaminants adhere to the surface. The adsorption capacity degradation can be minimized by modifying the pre-filters and fine dust filters. However, the worst-case scenario in which the filter may not play an effective role in the air purifier because of gaps, manufacturing errors, or other causes should be considered. Fine particles are removed by the filter, but moisture may not be removed. Moisture-containing indoor air degrades the adsorbent performance and competes with CO_2 during the adsorption process, reducing the performance [8]. The adsorbent is therefore used disposably and needs to be replaced periodically. Periodic filter replacement imposes an economic burden on consumers due to the continuous maintenance costs, and burdens the government with the nationwide environmental treatment cost for waste disposal. Some of the reported solutions use adsorbents that resist moisture [9–14] or employ

* Corresponding author.
E-mail address: ytkang@korea.ac.kr (Y.T. Kang).

https://doi.org/10.1016/j.jechem.2021.08.027

low-temperature regeneration to reduce the energy consumption [15,16]. These solutions are based on existing adsorbent materials.

Herein, we propose a new type of CO_2 capture material called liquid-like adsorbents (LLAs), which have the properties of liquid absorbents and solid adsorbents. LLAs are simple to manufacture and can be mass-produced. They can be applied in various methods and are capable of stable CO_2 capture. They are also safe for indoor use and are economical in the long term. Various evaluations of LLAs have demonstrated their potential as CO_2 capture materials.

2. Liquid-like adsorbents (LLA)

LLAs are a mixture of liquid and nanoscale solid particles (Fig. 1a). In the past, materials with such compositions were called nanofluids [17]. For the LLAs in this study, we used silicone oil for the liquid component and carbon nanotubes (CNTs) for the solid nanoparticles. CNTs have hydrophobic surfaces and cylindrical shapes that give them high bonding and oil absorption capacities. In addition, because CNT self-assembles into serpentine forms, it has excellent abilities for confining liquids into capsules as well as a large surface area that provides a large contact area with oil and, therefore, high bonding stability [18–20]. However, because CNT does not chemically bond with oil, the inherent properties of both the CNT and the oil are retained. This new type of CO_2 capture material can be expected to provide several advantages for indoor use. The LLA composition of moisture-resistant oil and CNTs can prevent performance degradation due to moisture. The thermally and structurally stable silicone oil and CNTs can be used for a long time. Physical CO_2 capture makes it easy to regenerate the adsorbent by increasing the temperature. The CNTs maintain the solidification of the LLA and allow the LLA with these adsorbent properties to be used as adsorbents. Moreover, because LLAs are not hard solids, it can be molded into various shapes and coated using oil onto sheets with excellent adhesion; therefore, LLAs can be used in various ways (Fig. 1b).

3. Experimental

3.1. Materials

All reagents were used as received from commercial suppliers without further purification. MWCNT (more than 90 wt% pure, Carbon Nano-material Technology Co., Ltd.), ethanol (anhydrous 99.5%, DEAJUNG), poly vinyl alcohol (PVA, Mw 31 000–50 000, 87%–89% hydrolyzed, Sigma Aldrich), and silicone oil (1000 cs, dimethylsiloxane structure, Saehan Silichem Co., Ltd) were used.

3.2. Preparation of LLAs based on CNT/silicone oil

Step 1: The CNTs were mixed with 200 mL of ethanol. The CNT concentration was calculated based on the amount of silicone oil that was added in a later step (200 g). PVA was added as a dispersion stabilizer at 1:1 ratio to the mass of the added CNT. The mixed solution was homogenized by ultrasonication (1 h, 20 Hz) and stirring.

Step 2: 200 g of silicone oil was mixed with the solution prepared in Step 1. Because of the high oil viscosity, a mechanical stirrer at 600 rpm was used for 1 h.

Step 3: Ethanol and moisture that might be included in the manufacturing process and the CNT dispersion were removed using a convection oven (24 h, 110 ℃).

Step 4: Vacuum treatment was performed to remove gas impurities. To prevent separation, the liquid was kept at 0.5 bar instead of an ultra-high vacuum for 6 h, and the performance of the finished sample was evaluated. The detailed preparation of the LLA adsorbents based on CNT/silicone oil is shown in Supporting Information Fig. S1 and Note S1.

3.3. Characterizations

The thermal conductivity k was calculated as

$$k = \alpha C_p \rho \quad (1)$$

where α, C_p, and ρ are the thermal diffusivity (NETZSCH, LFA 447 Nanoflash), specific heat (TA Instruments, DSC25), and density (HANSUNG, Chemical Balance), respectively. The value of each quantity was evaluated three times at 25 ℃. To measure the specific heat, the temperature was maintained at −5 ℃ for 5 min and then increased from −5 to 30 ℃ at the rate of 5 ℃ min^{-1}. The temperature of 30 ℃ was then maintained for 5 min. The surrounding gas was N_2. The density was determined by calculating the ratio between the measured weight (g) and volume (mL). A Quanta FEG 240 from FEI Corp. was used to obtain the field emission scanning electron microscopy (FE-SEM) image. Pretreatment was performed using a Pt target at 20 mA for 30 s (the materials did not contain elements with properties similar to those of Pt). The components were analyzed using the TEAM software suite from EDAX in conjunction with the FE-SEM. The component ratio was estimated by averaging the values obtained over three measurements for each resolution. Transmission electron microscope (TEM) measurements is evaluated by FEI's Tecnai G^2. The image solution was 0.23 nm or less, the accelerating voltage was 50–200 kV, and the magnification was in the range of 25–1,030,000. The structural characteristic of CNT in LLA was analyzed using a cryogenic transmission electron microscope (cryo-TEM) (Tecnai G2 Spirit TWIN, FEI Company

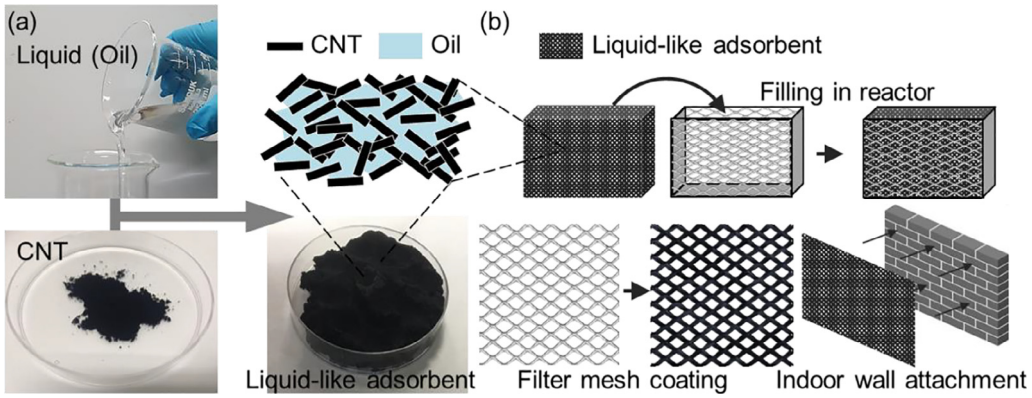

Fig. 1. Concept of liquid-like adsorbents. (a) Structure of LLAs. (b) Various methods of application of LLAs.

owned by Korea Advanced Institute of Science and Technology). The cryo-transfer holder (TH_626, Gatan Company) is used for cryogenic treatment. A rotational rheometer (TA Instruments Ltd., ARES-G2) was used to measure the viscosity. The shear rate sweep between 0.1 to 900 s^{-1} was analyzed, and the temperature was maintained at 25 ℃. The minimum transducer torques in oscillation and in steady shear were 0.05 μN·m and 0.1 μN·m, respectively. The maximum transducer torque, transducer torque resolution, strain resolution at the drive motor, and measurement gap were 200 mN·m, 1 nN·m, 0.04 μrad, and 1.0 mm, respectively. The measurement geometry was a 25 mm plate. The viscosity was analyzed at temperatures from 10 to 100 ℃ at a heating rate of 5 ℃ min^{-1} (shear rate: 10 s^{-1}).

3.4. Air collision resistance

The samples were prepared by applying the LLA to a 2 cm × 2 cm area on an Al plate, which is the main material in commercial filter meshes. The air collision direction was classified as either the front or the side based on the direction in which the LLA was applied. The maximum air velocity of the circulation fans used at homes was measured to be 5 m s^{-1}. The flow rate was therefore varied between 2 to 5 m s^{-1}. After the initial weight of the LLA was measured, the loss rate was computed by measuring the weight of the LLA after exposure to the air velocity for 30 min. A HEPA-class filter was used to prevent dust contamination from entering the fan, and the evaluation was conducted inside a hood. The detailed experimental information is shown in Supporting Information Fig. S2, Tables S1 and S2.

3.5. CO_2 capture capacity measurements

A homemade quasi-static pressure apparatus rated for 20 bar pressure and 150 ℃ temperature was used to measure the gas capture following a previously described procedure [21]. A schematic of the apparatus used is shown in Supporting Information Fig. S3. The apparatus consisted of a CO_2 capture chamber and a CO_2 reservoir tank made of stainless steel 304. The 0.3 L CO_2 capture chamber and the CO_2 reservoir tank were used to hold pure CO_2. These parts were connected to each other using high-pressure pipes and valves. The device was designed so that the operator could perform leak tests to ensure that there were no leaks in the system. After the LLA was prepared, the CO_2 capture tank was disconnected from the device, filled with 30 g of LLA, and then reconnected to the device. When valves 1, 2, and 3 were opened, air was removed from the inner container and the pipeline by a vacuum pump. After all the valves were closed, the CO_2 reservoir tank was filled with 2 bar of CO_2 gas from the CO_2 gas cylinder using the regulator. All the equipment was kept in a constant-temperature chamber for approximately 30 min to ensure an equilibrium temperature of 25 ℃. Then, CO_2 was injected into the CO_2 capture chamber from the CO_2 reservoir tank by connecting them to valves 1 and 3. As soon as the CO_2 pressure in the measuring tank reached the desired value, the valve was closed, and the pressure in the CO_2 capture tank was measured with a calibrated pressure gauge. To calculate the CO_2 capture capacity of the LLA in each experiment, the following assumptions were made: (1) The amount of air after the vacuum treatment was negligible. (2) The volume of the LLA did not change during the CO_2 capture. (3) The LLAs were initially free from CO_2. A mass balance was used to calculate the gas-phase CO_2 capture capacity under these assumptions. The initial and final number of moles of CO_2 in the tank were determined by measuring the temperature and pressure. The CO_2 capture capacities of the LLAs at equilibrium and at each time during the experiments was calculated as follows: Equilibrium was considered to be reached when no more than 0.001 bar of pressure change occurred in 1 h. All tests were performed at the constant temperature of 25 ℃.

$$\Delta n = n_0 - n_t \tag{2}$$

$$\Delta n = \frac{V_g}{RT}\left[\left(\frac{P_{CO_2}}{z_{CO_2}}\right)_0 - \left(\frac{P_{CO_2}}{z_{CO_2}}\right)_t\right] \tag{3}$$

$$\alpha = \frac{\Delta n}{m_{sample}} \tag{4}$$

where n_0 and n_t respectively denote the initial moles of CO_2 and the moles of CO_2 present in the gas phase at each time in the reactor, and $(z_{CO2})_0$ and $(z_{CO2})_t$ respectively represent the compressibility factors of the CO_2 in the gas phase calculated using the Soave–Redlich–Kwong (SRK) equation of state at the start and at each time period of the experiment. R and T are the universal gas constant and the temperature, respectively. m_{sample} is the mass of the LLAs, $(P_{CO2})_0$ and $(P_{CO2})_t$ are the initial pressure and pressure at each time period, respectively, and α is the amount of CO_2 captured. The experimental errors in the measurement of the temperature, pressure, volume, and weight were 1.25%, 0.11%, 0.04%, and 0.13%, respectively. The experimental uncertainty was calculated as per Abernethy et al. [22] and estimated to be within 1.26%. Detailed information on the experiment is listed in Supporting Information Note S2, Tables S3 and S4. The regeneration of the LLAs was performed for 3 h at the regeneration temperature, which was maintained using a convection oven. After the regenerated LLAs have cooled to 25 ℃, the regeneration ratio was confirmed by evaluating the CO_2 re-capture capacity.

3.6. Water capture measurements

The water capture measurements were carried out following a previously described procedure [23–25]. All measurements were performed at 25 ℃. The sample (5 g) was first immersed in deionized (DI) water (200 g). The sample was then removed from DI water, held for 30 s to allow the residual surface water to drip away, and then weighed. The water sorption of the LLAs were investigated by placing the LLA on the surface of the DI water and then measuring the weight of the LLA as a function of the sorption time. The procedure was repeated at intervals of 5–240 s. The water capture capacity of the LLA is expressed in weight of the DI water absorbed per weight of LLA (g g^{-1}):

$$Q_t = \frac{m_t - m_0}{m_0} \tag{5}$$

where Q_t (g g^{-1}) is the water capture capacity of the sample at a certain time, m_t (g) is the weight of the sample after water capture, and m_0 (g) is the initial weight of the sample.

3.7. Energy consumption analysis

The energy consumed in a system in which the LLAs are applied comprises the energy used by the fans to generate the air flow and the heating energy for regenerating the LLAs. The energy used by the fans, which are already configured parts of the system, has no effect and can be ignored. The differential pressure that results from applying the LLAs can affect the fan power, but this issue can be solved through the structural design of LLAs with high formability. The energy consumption per amount of CO_2 captured E (Wh mmol of CO_2 captured^{-1}) was therefore analyzed using the ratio of the energy consumed in the regeneration process to the CO_2 capture capacity:

$$E = \frac{Q_{reg}}{m_{CO2}} \tag{6}$$

where Q_{reg} (Wh) is the energy consumption for the LLA regeneration process, and m_{CO2} (mmol) is the amount of CO_2 captured.

4. Results and discussion

4.1. Characteristics of LLAs

CNTs have a high aspect ratio and a fiber-like shape (Fig. 2a and b). Other information on the CNTs, such as their diameter and density, are shown in Table S5 and Figs. S4 and S5. The high-viscosity silicone oil used as the liquid component of the LLAs in this study spread like water when dropped on a slide glass, but did not spread when more than 3 wt% of CNT was added to it (Fig. 2c). At the CNT concentration of 5 wt%, it became possible to solidify and mold the silicone oil; therefore, its viscosity and thermal properties at this concentration were investigated in this study. The viscosity of the LLA increased by 451.8 times at the shear rate of 1 s^{-1}, 59.0 times at the shear rate of 10 s^{-1}, and 27.7 times at the shear rate of 100 s^{-1} (Fig. 2d). At 5 wt% LLA, the viscosity decreased as the shear rate increased. This resulted in a pseudoplastic fluid and shows that the silicone oil can be used as a solid-like adsorbent. When solid particles with high thermal conductivity were added to the fluid, the heat transfer performance of the LLA improved. Thermal energy is required to regenerate the LLA after CO_2 capture. The CO_2 regeneration and long-term CO_2 capture performance of the LLA can thus be maintained by improving the heat transfer performance. The addition of CNT to the silicone oil improved its thermal conductivity, thermal diffusivity, and specific heat by 25.8, 89.0, and 1.36 times, respectively (Fig. 2e). This is a dramatic improvement of the heat transfer properties over the nanofluids in other studies (a 1.1–2.6 times increase in thermal conductivity was reported [26]). This result indicates that the LLA is more similar to a nanocomposite than to a nanofluid, which is a reasonable result based on the thermal conductivity improvement model for nanocomposites [27,28] (see Supporting Information Note S3 for more details). The improvement of the heat transfer in the LLAs can be attributed to phonon transport and the percolation network mechanism. In LLA, heat is transferred by nanoparticles and by phonons. Phonons are the primary heat carriers in non-metallic materials. The non-metallic material transfers heat through lattice vibrations because its atoms are close to one another [29]. Although phonon is a wave concept, it is also considered a quantum concept for describing heat transfer in non-metallic materials [30]. The low thermal resistance due to the percolation network is also an important reason for the improved heat transfer performance in LLAs. The interfacial thermal resistance, known as the Kapitza resistance at the solid-medium boundary, interferes with heat transfer [31]. To improve the heat transfer, a thermal path that is not affected by the Kapitza resistance is required. When the concentration of added nanoparticles exceeds a threshold, the nanoparticles form a continuous electrically conductive network. The formation of the network is facilitated by the larger aspect ratio of CNTs compared to spheres [32]. This phenomenon improves the heat transfer performance because heat is transferred by the percolation network rather than by the fluid.

4.2. Feasibility of LLAs for indoor use

Scattered LLAs can enter the human respiratory tract and may cause harmful effects to health. The thermal stability and air collision resistance of LLAs were studied to evaluate the potential of LLAs for indoor applications. To confirm the thermal stability of LLAs, the weight loss was determined by thermogravimetric analysis (TGA) (Fig. 3a). The temperature of the evaluation sample was raised to 800 ℃ in ambient environment exposed to air. Weight loss in silicone oil began to occur at 208 ℃, whereas for the samples with 5 wt% CNTs added, weight loss began to occur at 279 ℃. (The starting point of the weight loss was defined as the point when the sample reached 99.9% of its initial weight.) The reduction in the maximum weight loss signifies an increase in the thermal stability of silicone oil due to the addition of CNTs. Many studies have shown that thermal stability is improved by the intermolecular forces between CNTs and oil [33–35]. Although silicone oil alone is stable enough to be used indoors [36], it has been shown that the addition of CNTs can further enhance its thermal stability.

The air collision resistance of the LLAs was evaluated by attaching LLAs to an Al plate and exposing them to air velocity (Fig. 3b). When air collided with the front of the LLAs, no weight loss occurred regardless of the thickness of the adhered LLAs (1 to 6 mm). However, when air collided with the LLAs from the side,

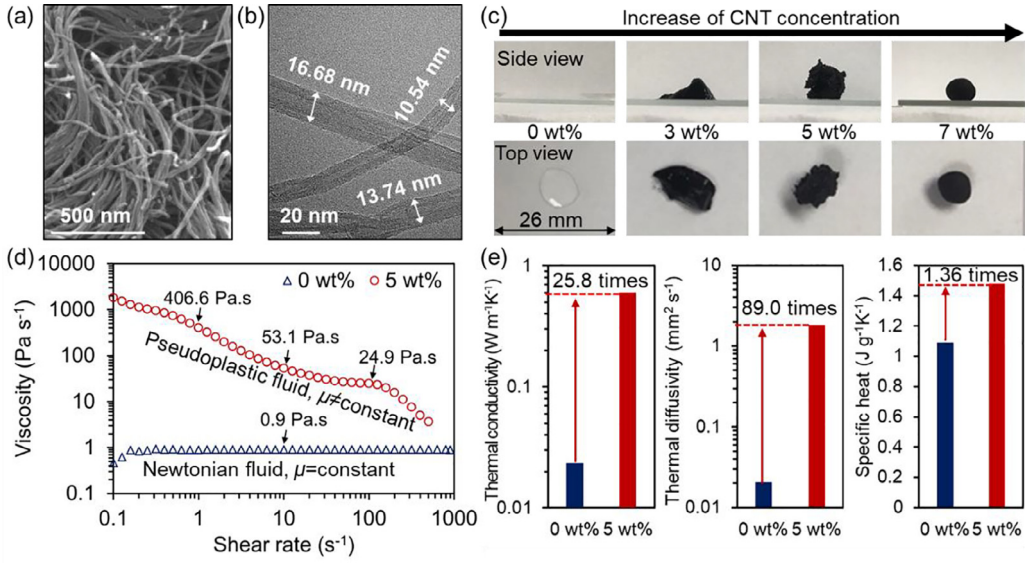

Fig. 2. Properties of silicone oil after the addition of CNT. (a) SEM image of the CNT. (b) TEM image of the CNT. (c) Shape of the LLAs prepared according to the CNT concentration. (d) Viscosity of the LLAs at 0 wt% and 5 wt% concentration of the added CNT according to the shear rate. (e) Thermal properties of the LLAs at 0 wt% and 5 wt% concentration of the added CNT.

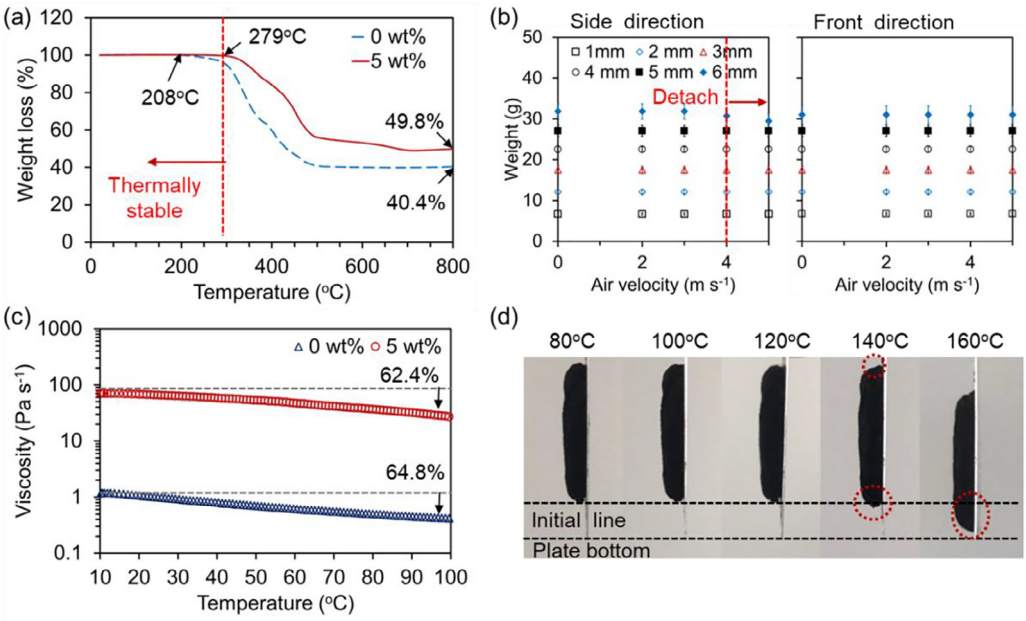

Fig. 3. Feasibility test of the LLAs for indoor use. (a) Weight loss of the LLAs at 0 wt% and 5 wt% concentration of the added CNT by TGA. (b) Weight loss of the LLAs at 0 wt% and 5 wt% concentration of the added CNT according to the air velocity. (c) Viscosity of the LLAs at 0 wt% and 5 wt% concentration of the added CNT according to the temperature. (d) Adhesion of LLAs at 0 wt% and 5 wt% concentration of the CNT according to the temperature.

the weight of the 6 mm-thick LLA decreased at the air velocity of 4 m s^{-1}. The loss occurred not at where the LLA decomposed, but rather at the edge of the LLA attached to the Al plate. The edge is more susceptible to air collisions because of its exposure to the air. In addition, the critical thickness of the attachment is 6 mm, whereas the thickness of the attachment in general use is 2 mm or less [37]. The LLA can therefore be used reliably indoors because household circulation fans (18 inch (45.7 cm)) operate at 4.5 m s^{-1} [38].

Heating is required for LLA regeneration. As the temperature rises, the viscosity of the LLAs decreases because of the decrease in the intermolecular attraction. In this study, the LLA is a non-Newtonian fluid because of its increased viscosity due to the addition of CNT, but it becomes a Newtonian fluid when the temperature increases. If it becomes a fluid because of a decrease in viscosity, the adsorbent property of the LLA will be lost and the performance of the system will be degraded. When the temperature was increased from 10 ℃ to 100 ℃, the viscosity decreased by approximately 60% regardless of whether CNT was added (Fig. 3c). However, because the increase in the LLA viscosity due to the addition of CNT was larger than the viscosity reduction due to the temperature increase, the viscosity was maintained within a stable range. The changes induced by heating LLA attached to an Al plate were visually observed (Fig. 3d). When the temperature was increased to 120 ℃, the LLA changed visually independently of the change in viscosity. The LLA sagged at 140 ℃ and the contact angle between the top and bottom changed. The temperature could not be maintained at 160 ℃ because the LLA would slip along the plate. These results confirm that LLA can be used stably indoors without scattering. In addition, they confirm that the temperature limit for adhesion stability is 120 ℃, and that the maximum regeneration temperature of the sample should be kept below 120 ℃ regardless of the thermal stability of the sample.

4.3. CO_2 capture in LLA

The CO_2 capture capacity of LLAs with different concentrations of added CNT was evaluated (Fig. 4a and b). The measured CO_2 capture capacities of the LLAs were 0.120, 0.117, 0.129, and 0.134 mmol g^{-1} for the CNT concentrations of 0, 3, 5, and 7 wt%, respectively. When 3 wt% CNT was added, the CO_2 capture capacity of the LLA decreased by 4.5% compared to when no CNT was added. This is because when CNT is added, the amount of silicone oil is reduced by that amount. The CO_2 capture capacity tends to increase from 5 wt% of the CNT concentration, which seems to be because the effect of improving mass transfer due to the addition of CNTs is superior to the effect of reduced the amount of silicone oil. However, after the addition of 5 wt% CNT, the CO_2 capture capacity increased compared to when no CNT was added. When 7 wt% CNT was added, the CO_2 capture capacity increased by 11.5%. Although the mechanism for mass transfer enhancement through the addition of nanoparticles to an absorbent has not been clearly identified, bubble destruction, interfacial mixing, and shuttle effects have been suggested as possible mechanisms [39]. The bubble destruction and interfacial mixing effects result from the convective motion of the nanoparticles. Spherical particles can exhibit random free motion along multiple directions in a fluid, but the gas–liquid mixing effect may be small because the rod-shaped CNTs possess relatively small degrees of freedom. In addition, because the LLA has high viscosity, it can be expected that the motion of the nanoparticles will not have significant effects. However, the shuttle effect [40,41], which depends on the surface adsorption/desorption of nanoparticles, may be applicable for the improved CO_2 capture rate in this study.

The CO_2 capture enhancement ratio is obtained by dividing the CO_2 capture capacity over time by the CO_2 capture capacity of the 0 wt% LLA (Fig. 4c). In the initial segment spanning the first 1000 s, the 5 wt% LLA showed a 1.23-fold improvement and the 7 wt% LLA showed a 1.54–3.25-fold improvement in the CO_2 capture capacity. This trend is confirmed more clearly through the CO_2 capture rate (Fig. 4d). The CO_2 capture rate means the CO_2 capture capacity variation per unit time (after 2000 seconds, all cases tend to converge to zero). The CO_2 capture rates of the LLAs were 15.794, 12.494, 19.391, and 31.271 $\times$ 10^{-5} mmol g^{-1} s^{-1} for the CNT concentrations of 0, 3, 5, and 7 wt%, respectively, during the initial 100 seconds. It shows that the capture rate is improved by

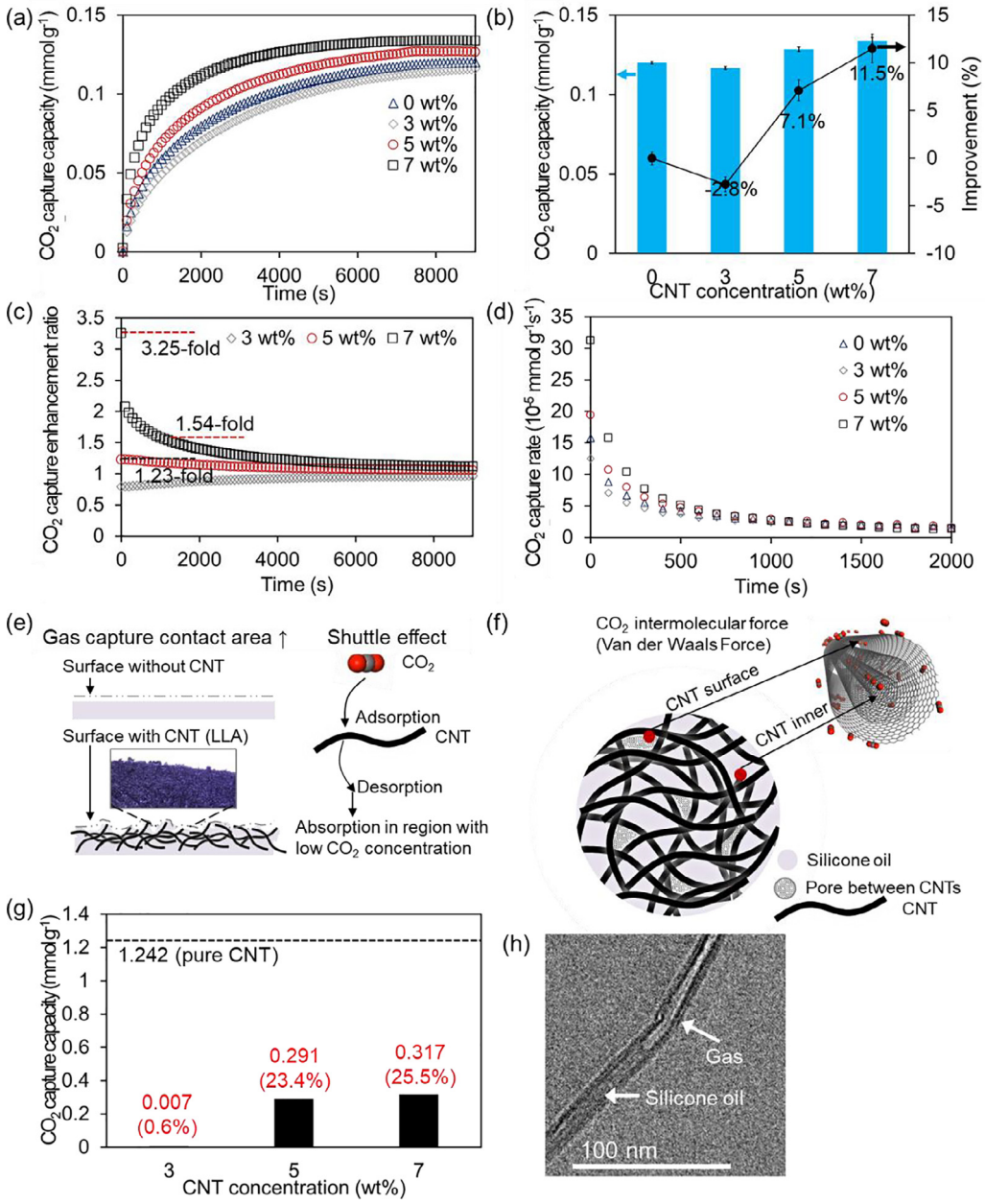

Fig. 4. CO_2 capture of the LLAs. (a) CO_2 capture capacity variation of the LLAs according to time during the CO_2 capture experiment. (b) CO_2 capture capacity of the LLAs according to the CNT concentration. (c) CO_2 capture enhancement ratio of the LLAs according to time during the CO_2 capture experiment. (d) CO_2 capture rate of the LLAs according to the CNT concentration. (e) CO_2 capture acceleration model of the LLAs. (f) CO_2 capture capacity enhancement model of the LLAs. (g) CO_2 capture capacity of CNT in the LLA. (h) Cryo-TEM image of CNT in LLA (measured by diluting a sample of LLA at 7 wt% concentration of the added CNT in a 1:20 weight ratio with DI water).

CNTs when LLA is used in a continuous capture process before the saturated capacity. These results prove the enhancement of CO_2 mass transfer performance by CNTs. When the CO_2 concentration in the LLA was low, the large difference in the CO_2 concentration between the inside and outside of LLA accelerated the CO_2 transport by the CNTs. As the CNTs began to saturate, the degree of improvement decreased along with the concentration difference. In addition, the CO_2 capture was affected by the gas contact area. When the CNT concentration exceeded 5 wt%, CNTs became exposed on the surface of the LLA and the surface became rougher than that of the liquid (Fig. 4e; see Supporting Information Fig. S6 and Note S4 for more details). The large surface area of the nanostructured surface increases the gas contact area [42,43], which in turn increases the CO_2 capture rate. Although these phenomena can increase the rate of CO_2 capture, they cannot explain the increase in the amount of CO_2 captured. Because the proportion of silicone oil decreased with increasing CNT concentration, the CO_2 capture capacity would be expected to decrease, but it increased instead. This implies that the CNTs are directly involved in CO_2 capture.

Physical adsorption can occur both on the surface of a CNT and inside a CNT through the van der Waals force (Fig. 4f) [44,45]. Many studies have shown that the CO_2 capture performance of an absorbent improves when it contains CNTs [21,46–49]. Molecular dynamics simulations confirm that when CNT and silicone oil are blended, the van der Waals force increases, which can improve the CO_2 capture capacity (see Supporting Information Note S5, Fig. S7, and Table S6 for more details). In this study, the CO_2 capture capacity of the CNT used was 1.242 mmol g^{-1} (see Supporting Information Fig. S4 for more details). The CO_2 capture capacities of

the CNT in LLA were 0.007, 0.291, and 0.317 mmol g^{-1} for the CNT concentrations of 3, 5, and 7 wt%, respectively (Fig. 4g), which means the CO_2 capture capacities of the CNT in the LLA decreased by 99.4% (0.007 mmol g^{-1}), 76.6% (0.291 mmol g^{-1}) and 74.5% (0.317 mmol g^{-1}) for CNT concentrations of 3, 5 and 7 wt%, respectively. Although the CO_2 capture capacity of the CNT decreased when oil and CNT were blended, the LLAs of 5 and 7 wt% still showed 23.4 and 25.5% of the capacity of the pure CNT, respectively.

In this study, the LLAs did not come into full contact with the silicone oil and all sides of the CNTs. Therefore, the density of the LLA decreased when the concentration of the added CNTs decreased (see Supporting Information Fig. S8 for more details). This implies that voids are created when the CNTs assemble and the porosity of the LLA is increased. In addition, oil enters the interior of the CNTs because of the capillary effect although the effect is reduced by the non-uniformity of the CNT diameter and the serpentine, rather than straight, line shape of the CNTs, which makes it difficult to completely fill the CNTs with liquid [50,51]. It was confirmed that the silicone oil was absorbed in the CNT in the LLA, and it was not shown that the inside of the CNT was not completely filled (Fig. 4h; see Supporting Information Fig. S9 for more details). The CNT in silicone oil can also capture CO_2 and further increase the total CO_2 captured by creating voids in the LLA at higher concentrations of CNT. The addition of 3 wt% CNT did not have a significant effect on the CO_2 capture because of the low CNT concentration and small number of internal voids created, but the CO_2 adsorption capacity increased by 23%–25% in LLA with 5 and 7 wt% CNT. The change in the morphology of the LLA due to the addition of CNT is related to CO_2 capture. When CNTs are added and the morphology of the LLA changes, the CO_2 capture capacity of the CNT increases. For the oil and particle combination used in this study, the concentration threshold is between 3 and 5 wt%.

Based on the results in this section, the mechanisms of CO_2 capture process in the LLA are summarized as follows;

(1) Reactivity of absorbent with CO_2: The physical absorbents such as silicone oil, used in this study, CO_2 is captured depending on solubility. If the chemical absorbents such as MEA or PEI are used, CO_2 is captured by chemical bonding with the amine group. Since the main component of LLA is an absorbent that is a liquid, most of its CO_2 capture capacity is determined by the reactivity of absorbent with CO_2.
(2) Adsorption by solid particles (Fig. 4f): In physical adsorption, CO_2 is bound to the surface by van der Waals forces with the adsorbent. Chemisorption process can occur if chemical functional groups such as amine groups are applied to the adsorbent surface. In addition, in the case of CNT particles used in this work, it was confirmed that 23–25% of the adsorption area was preserved due to the micropores generated during the self-assembly process despite being mixed with the absorbent (Fig. 4g).
(3) Changes in LLA interface properties by solid particles (Fig. 4e): When more than the threshold concentration of solid particles is added to the liquid absorbent, it is exposed to the surface, and the LLA-CO_2 contact surface changes from a smooth state to a rough state. The absorbent-adsorbent composite surface formed by the CNTs, the particles used in this study, increases the CO_2 contact interface by the microscale roughness. CNTs exposed on the surface are also directly involved in CO_2 capture and shuttle. This phenomenon contributes to reaching the saturation condition rapidly as it promotes the initial mass transfer performance of CO_2.

4.4. Regeneration of LLAs

To regenerate the LLAs, CO_2 desorption was carried out by heating. Because the CO_2 was captured by physical absorption/adsorption, the regeneration ratio increased with the temperature (Fig. 5a). When 3 wt% CNT was added to the LLA, the LLA regeneration showed no significant difference from that of pure silicone oil; however, at CNT concentrations above 5 wt%, the LLA regeneration ratio increased. This effect was even more pronounced when the LLA was regenerated at lower temperatures. The solubility is a thermodynamic property and a function of temperature; therefore, it must take a constant value at a given regeneration temperature. However, the addition of CNT seems to increase the regeneration ratio because of the desorption of CO_2 trapped in the CNT. When a fluid that contains nano-scale particles is attached to or immersed in a heat transfer surface, the particles are deposited on the surface (Fig. 5b). The absorbed gas nucleates on irregular and rough surfaces. The deposition of nanoparticles facilitates bubble nucleation by increasing the density of nucleation sites [52,53]. The improved heat transfer allows the LLA to reach the regeneration temperature faster (Fig. 2f and 5b). The rapid generation of CO_2 bubbles can affect the regeneration ratio and accelerate the regeneration. CO_2 is desorbed in the form of bubbles in silicone oil because of the high oil viscosity, but the CO_2 bubbles may not have enough buoyancy to raise and be discharged because of the strong viscous force. Therefore, the bubbles must be given momentum through rapid bubble generation to allow them to escape from inside the high-viscosity fluid. The viscosity of the LLAs in this study increased after the addition of CNTs, but because the LLAs have porous structures, there are paths through which the generated air bubbles can pass. These paths and the hollow pores of the CNTs create frictionless pathways for ultrahigh transport rates [54,55] and allow the regenerated CO_2 gas to be expelled easily to the atmosphere (Fig. 5c). The right side of Fig. 5c shows the regeneration of CO_2 by immersing the LLA after CO_2 capture in hot water at 80 ℃. The CO_2 capture performance was maintained at 95% even after the CO_2 capture/regeneration process was repeated for 20 cycles (Fig. 5d). This is because the CO_2 capture is a physical gas transport process. Because there is no chemical reaction, the CO_2 capture is stable for extended periods of time, and regeneration is possible at a low temperature. In addition, the CO_2 capture/regeneration cycle was evaluated once per day for total 20 days. The stability of LLA was confirmed by measuring the density variation with respect to time during the cycle tests, and it was found that LLAs of 5 and 7 wt% were stable for 20 days. In the case of LLA of 3 wt%, it was confirmed that the stability was not maintained for only 7 days because CNT could not handle all the silicone oil, and some oil was separated (see Supporting Information Fig. S8 for more details). However, in the cases of 5 and 7 wt% in which the solidification process was sufficiently advanced, it was confirmed that the density was maintained constant by the self-assembly effect of CNTs.

4.5. Water resistance

The air in the room is humid. The humidity varies widely with the season and region (annual relative humidity range in Seoul, South Korea: 17.9%–96.3% [56]). Moisture and CO_2 physically compete each other during the adsorption process in the same space. When the water vapor pressure in the adsorbent increases, it desorbs CO_2 while adsorbing more water molecules. Water resistance effect is an important factor because isolated carbonate ion hydrations during the water and CO_2 sorption process causes CO_2 binding and release [8]. In this study, the water capture capacity of the LLAs is investigated because it can affect the CO_2 capture capacity.

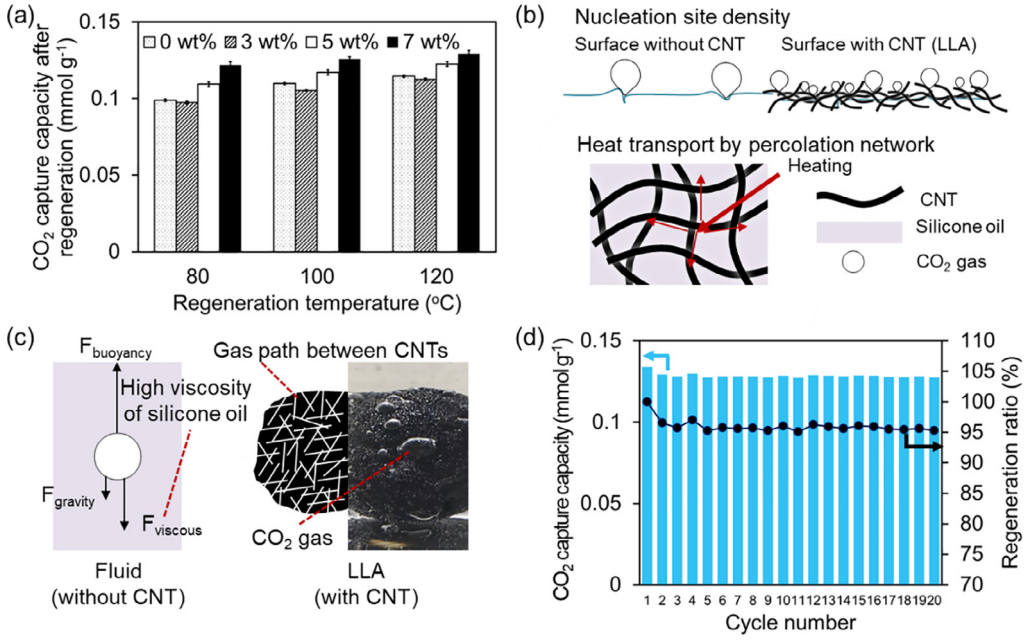

Fig. 5. Regeneration of LLAs. (a) CO_2 capture capacity of the LLAs according to CNT concentration and the regeneration temperature after the regeneration process. (b) CO_2 regeneration enhancement model in CNT. (c) CO_2 regeneration acceleration model of the LLAs. (d) Durability of the LLA due to the repeated CO_2 capture/regeneration cycles (CNT concentration: 7 wt%, regeneration temperature: 120 ℃).

The water capture capacities of the LLAs were 0.008, 0.018, and 0.02 g g^{-1} at the CNT concentrations of 3, 5, and 7 wt%, respectively. The water capture capacities increased with the CNT concentration (Fig. 6a). The 3 wt% LLA, which had a low CNT concentration, had a smooth surface, but the surfaces of the 5 and 7 wt% LLAs were rough (see Supporting Information Fig. S6 for more details). Therefore, in the 5 and 7 wt% LLAs, the water that adhered to the surface did not fall off and the amount of water captured increased. However, the water captured was not due to the absorption of water inside the LLA but rather, due to the water that remained on the surface. After natural drying, all the water on the surface disappeared and the weight of the LLA returned to its original value. Even when water was dropped on the surface of the LLA, the LLA exhibited hydrophobic behavior (Fig. 6a). The LLAs were treated with water in the above manner and their CO_2 capture capacity was evaluated. To analyze the effect of water, only the weight of the LLA and not that of the water captured was considered. The CO_2 capture capacity increased by 0.0003 (0.28%), 0.0007 (0.6%), and 0.0008 (0.6%) mmol g^{-1} at the CNT concentrations of 3, 5, and 7 wt%, respectively (Fig. 6b). Because these increases were within the experimental error range (<1.26%, see Supporting Information Note S2 for more details), it cannot be concluded that water adhesion to the LLAs had an effect on the CO_2 capture capacity. However, the results clearly show that water does not degrade the LLA CO_2 capture capacity. The CO_2 capture capacity of a solid adsorbent with a porous surface will be degraded when water removes the pores that capture CO_2. However, because the CO_2 is captured through solution by the liquid absorbent in the LLAs, the CO_2 capture is unaffected by moisture surface contamination. This characteristic of the LLAs allows a blower to be used to remove the moisture deposited on the LLA surfaces by the inflow of wet air and the reaching of the dew point.

4.6. Energy consumption analysis

The energy consumption per CO_2 capture was analyzed using the ratio of the energy consumed during the regeneration process to the amount of CO_2 captured. Regeneration energies of 598, 413,

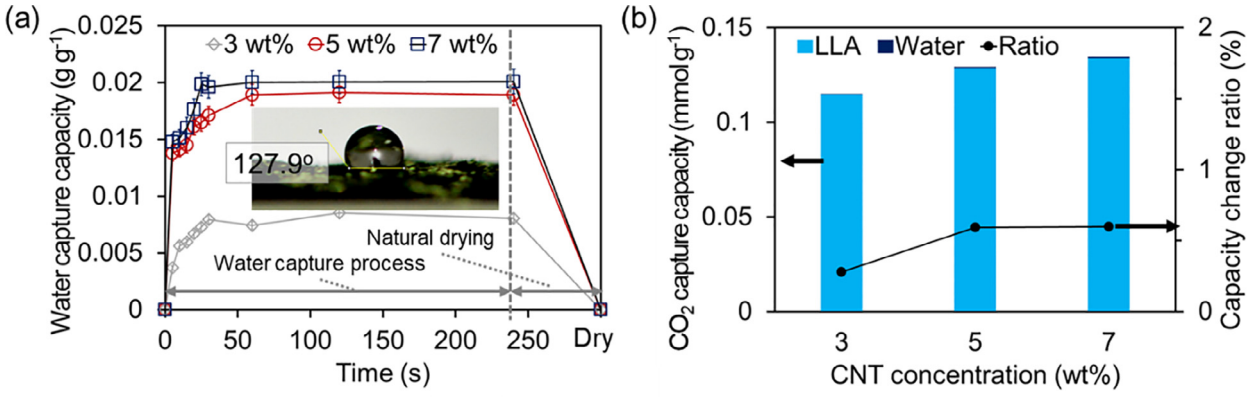

Fig. 6. Water resistance of the LLAs. (a) Water capture capacity of the LLAs according to the CNT concentration (center image is the contact angle of the water droplet on the surface of the 7 wt% LLA). (b) CO_2 capture capacity of the LLAs after being soaked in water.

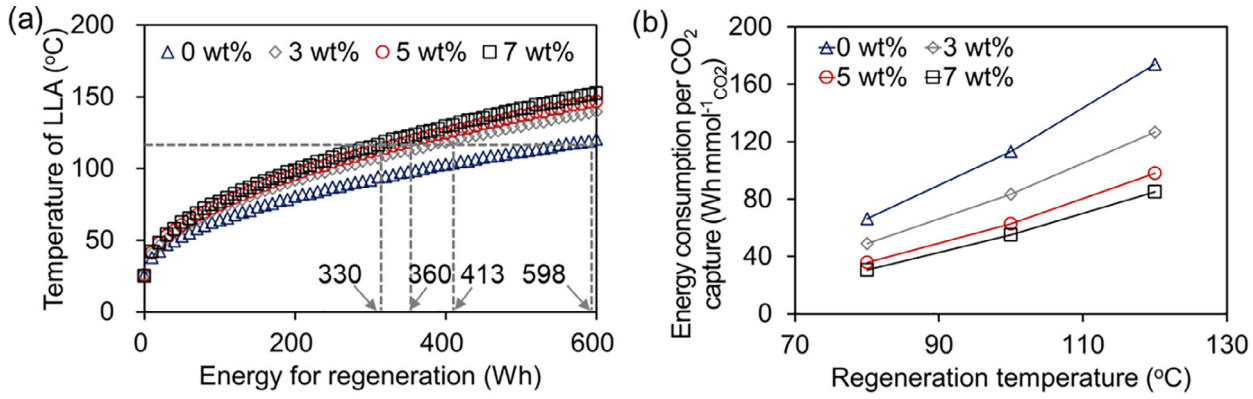

Fig. 7. Relationship between the CO_2 capture capacity and the energy consumption according to the CNT added. (a) Temperature of LLAs according to energy consumption for regeneration. (b) Energy consumption per amount of CO_2 captured according to the regeneration temperature and the concentration of the added CNT.

Table 1
Comparison of CO_2 capture capacity onto various adsorbents.

Adsorbents	CO_2 capture capacity (mmol g^{-1})	Temperature (℃)	CO_2 concentration (%)	Ref.
Kaolinite-H_2SO_3	0.08	25	100	[61]
Zeolite 13X	0.03	25	15% (wet)	[62]
	3.18	25	15% (dry)	
CNF[a]-silica aerogels with 30% APTES[b]	1.49	25	100	[63]
Fibrous MgO-SiO_2	2.48	75	60	[64]
N-enriched hierarchically porous carbon nanosheets	2.5	25	100	[65]
PEI@BN[c]	3.12	75	2	[66]
UiO-66(Zr)-NH_2-F_4	0.76	25	15	[9]
5A@MSAs[d]	5.05	25	15	[10]
5A@ZIF-8	2.67	25	15	[13]
MDC[e]	1.54	22	15	[14]
MgO-RHA[f]	4.56	25	10	[67]
FBNNSs[g]/ZnO	2.83	0	100	[68]
Aminopolymer impregnated MCM-36	0.27	25	100	[69]
NOHM-I-PEI[h]	1.7	25	0.04	[12]
PEI-MR10	2.918	25	0.1	[15]
LLAs[i] (7 wt% CNT)	0.134	25	100	This work

[a] CNF: Cellulose nanofibrils. [b] APTES: (3-Aminopropyl)triethoxysilane. [c] PEI@BN: Polyethyleneimine functionalized boron nitride nanosheets. [d] MSAs: Mesoporous silica-supported-amine hybrids. [e] MDC: Microporous dominated carbon. [f] RHA: Rice husk ash. [g] FBNNSs: Functionalized boron nitride nanosheets. [h] NOHM-I-PEI: Nanoparticle organic hybrid materials functionalized with polyethylenimine. [i] LLAs: Liquid-liked adsorbents.

360, and 330 Wh were respectively required for the CNT concentrations of 0, 3, 5, and 7 wt%, after the temperature of 120 ℃ was reached (Fig. 7a). These results show that the energy consumption for LLA regeneration decreases with increasing CNT concentration. Because the LLA regeneration process occurred in the actual environment where there was heat loss due to the ambient temperature, the reduction of energy consumption was not as significant as the improvements in the thermal conductivity and the heat diffusion rate. Nonetheless, there was a sufficient improvement in the heat transfer performance. Fig. 7b shows the ratio of the energy consumption per amount of CO_2 captured according to the regeneration temperature and the CNT concentration. This method is generally used for energy consumption analysis in CO_2 capture systems. Energy is consumed in industrial processes for various purposes, such as for pumping, cooling, and heating [57,58], in this study, we considered only the energy for LLA regeneration in the system to which the LLA was applied. The CO_2 capture capacity was lower at 3 wt% CNT than at 0 wt% CNT (Fig. 4b), but the energy consumption per amount of CO_2 captured decreased because of the increased heat transfer. The energy consumption rate therefore decreased as the CNT concentration increased. In contrast, as the regeneration temperature increased, the LLA regeneration ratio improved. A large amount of CO_2 could be captured, but the energy consumption per amount of CO_2 captured increased because of the increase in the energy consumption ratio to increase the temperature. In a simple energy analysis, it is concluded that a high CNT concentration and a low regeneration temperature (80–120℃) are advantageous for reducing the energy consumption. This temperature grade can be regenerated without additional energy consumption when using a solar collector, and when applied to an HVAC system, CO_2 emission can be reduced without ventilation, which reduces the heating and cooling loads by reducing the frequency of ventilation, thereby contributing to energy saving within buildings.

4.7. Future studies

LLA is a new type of material that can reduce indoor CO_2. By adding CNTs to silicone oil, which is an absorbent, it can be molded into various shapes and used indoors. Although LLAs have a lower performance than bulk CNT, it has a higher bulk density than CNT, and it can exhibit the same performance with 1/3 of the CNT volume, so it can be applied to a limited indoor space. However, some related problems must be solved before they can be commercialized. One such problem is the high cost of CNT [59]. The cost is a common concern to all nanoparticle researchers. Moreover, in this study, a high concentration of CNT was added. Another problem is while the silicone oil studied here has excellent stability, its relatively low CO_2 capture capacity does not make it an attractive choice. The CO_2 capture capacity of LLA is about four times better

than that of water [60], similar or better than other adsorbent materials [61,62], but not good enough for the miniaturization of the system. The capacities of various adsorbents based on the recently studied 1D [63,64], 2D materials [65,66], nanostructured materials [9,10,13,14,67–69], and hybrid polymers [12,15] range from 0.76 to 5.05 mmol s^{-1} (Table 1) and therefore, the performance upgrades are required through future studies. Many previous studies have investigated oil-based CO_2 absorption [70–74]. The high viscosity of oil makes it an unattractive absorbent because the oil needs to be circulated using a pump. This study has shown that oil can be used as an adsorbent by solidifying it. Further studies are needed to find an eco-friendly oil with excellent CO_2 capture capacity. To promote the use of oil as an adsorbent in the future, oil with excellent CO_2 capture capacity and stability, hydrophobic sorbents other than CNT such as metal-organic framework (MOF) based composite [9,13], porous dominated carbon [14], porous resin [15], and the optimal combination should be studied. Finally, based on the upgraded LLA, a correlation analysis of humidity and CO_2 concentration will be performed by evaluating CO_2 capture performance under conditions of actual indoor low-concentration CO_2.

5. Conclusion

In summary, we investigated a new type for CO_2 capture in indoor environments. When the CNT concentration exceeded 5 wt% within the conditions of this study, the fluid solidified and became fixed like an adsorbent. The CNTs in the absorbent also contributed to the enhancement of CO_2 capture, the CO_2 capture capacity was improved by 11.5% when 7 wt% of CNT was added. The combination of oil and CNT has long-term stability (95% regeneration rate, maintains CO_2 capture performance for 20 cycles) and water resistance, and at the same time possesses the solubility properties of the absorbent and the solid properties of the adsorbent. Therefore, there is no surface clogging like conventional solid adsorbent due to contamination by moisture and dust contained in the indoor air, preventing performance degradation. In addition, the improved heat transfer due to the addition of CNTs reduces the consumption of renewable energy. Due to the improved heat transfer and regeneration performance, it is regenerated with a low-temperature heat source of 80 ℃, so it can be driven by solar heat instead of an electric heater. LLAs can provide a very simple alternative solution for indoor CO_2 reduction. They can be used to fill modules in the same way as conventional adsorbents and to coat demister filters, and also used as filters inside air purifiers. LLAs can also be applied to wall sheets and used directly for indoor CO_2 reduction. In a future study, the capacities of LLAs will be fine-tuned, and their capacity for specific applications is expected to be improved through the use of various oil and CNT combinations and functionalized CNT groups. Work is in progress to optimize these liquid adsorbents for actual air purifiers and industrial filters by exploring and testing the capacity upgrades of these materials in the system structures.

Declaration of Competing Interest

The authors declare that they have no known competing financial interests or personal relationships that could have appeared to influence the work reported in this paper.

Acknowledgments

This work was supported by the National Research Foundation of Korea (NRF) grant funded by the Korean government (MSIT) (Grant number: 2020R1A5A1018153 and No. 2020R1A6A3A01095950).

Appendix A. Supplementary data

Supplementary data to this article can be found online at https://doi.org/10.1016/j.jechem.2021.08.027.

References

[1] T.A. Jacobson, J.S. Kler, M.T. Hernke, R.K. Braun, K.C. Meyer, W.E. Funk, Nat. Sustain. 2 (2019) 691–701.
[2] X. Shi, H. Xiao, H. Azarabadi, J. Song, X. Wu, X. Chen, K.S. Lackner, Angew. Chem. Int. Edit. 59 (2020) 6984–7006.
[3] S.B. Kwon, W. Jeong, D. Park, K.T. Kim, K.H. Cho, J. Hazard. Mater. 297 (2015) 295–303.
[4] V. Martins, T. Moreno, M.C. Minguillon, B.L. van Drooge, C. Reche, F. Amato, E. de Miguel, M. Capdevila, S. Centelles, X. Querol, Environ. Pollut. 208 (2016) 125–136.
[5] B. Xu, J. Hao, Environ Int 107 (2017) 33–46.
[6] F. Wu, M.D. Argyle, P.A. Dellenback, M. Fan, Prog. Energy Combust. Sci. 67 (2018) 188–205.
[7] K. Fu, W. Rongwong, Z. Liang, Y. Na, R. Idem, P. Tontiwachwuthikul, Chem. Eng. J. 260 (2015) 11–19.
[8] X. Shi, H. Xiao, K. Kanamori, A. Yonezu, K.S. Lackner, X. Chen, Joule 4 (2020) 1823–1837.
[9] Z. Hu, A. Gami, Y. Wang, D. Zhao, Adv. Sustain. Syst. 1 (2017) 11.
[10] X. Liu, F. Gao, J. Xu, L. Zhou, H. Liu, J. Hu, Micropor. Mesopor. Mat. 222 (2016) 113–119.
[11] L.H. Xie, M.M. Xu, X.M. Liu, M.J. Zhao, J.R. Li, Adv. Sci. 7 (2020) 1901758.
[12] G. Rim, T.G. Feric, T. Moore, A.H.A. Park, Adv. Funct. Mater. 31 (2021) 2010047.
[13] F. Gao, Y. Li, Z. Bian, J. Hu, H. Liu, J. Mater. Chem. A 3 (2015) 8091–8097.
[14] J. Pokrzywinski, D. Aulakh, W. Verdegaal, V.H. Pham, H. Bilan, S. Marble, D. Mitlin, M. Wriedt, Adv. Sustain. Syst. 4 (2020) 2000001.
[15] W. Wang, F. Liu, Q. Zhang, G. Yu, S. Deng, Chem. Eng. J. 399 (2020) 125734.
[16] R. Rodriguez-Mosqueda, J. Rutgers, E.A. Bramer, G. Brem, J. CO2 Util. 29 (2019) 65–73.
[17] S.U. Choi, J.A. Eastman, Argonne National Lab., IL (United States), 1995.
[18] X. Gui, J. Wei, K. Wang, A. Cao, H. Zhu, Y. Jia, Q. Shu, D. Wu, Adv. Mater. 22 (2010) 617–621.
[19] X. Chen, N.S. Villa, Y. Zhuang, L. Chen, T. Wang, Z. Li, T. Kong, Adv. Energy Mater. 10 (2020) 1902769.
[20] D. Kukkar, A. Rani, V. Kumar, S.A. Younis, M. Zhang, S.S. Lee, D.C.W. Tsang, K.H. Kim, J. Colloid Interf. Sci. 570 (2020) 411–422.
[21] M. Nabipour, P. Keshavarz, S. Raeissi, Int. J. Refrig. 73 (2017) 1–10.
[22] R.B. Abernethy, R.P. Benedict, R.B. Dowdell, J. Fluid. Eng.-T. ASME 107 (1985) 161–164.
[23] M.M. Radetic, D.M. Jocic, P.M. Jovancic, Z.L. Petrovic, H.F. Thomas, Environ. Sci. Technol. 37 (2003) 1008–1012.
[24] D. Ceylan, S. Dogu, B. Karacik, S.D. Yakan, O.S. Okay, O. Okay, Environ. Sci. Technol. 43 (2009) 3846–3852.
[25] X. Gui, H. Li, K. Wang, J. Wei, Y. Jia, Z. Li, L. Fan, A. Cao, H. Zhu, D. Wu, Acta Mater. 59 (2011) 4798–4804.
[26] S.M.S. Murshed, C.A.N. de Castro, Renew. Sust. Energ. Rev. 37 (2014) 155–167.
[27] Z. Han, A. Fina, Prog. Polym. Sci. 36 (2011) 914–944.
[28] Y. Guo, K. Ruan, X. Shi, X. Yang, J. Gu, Compos. Sci. Technol. 193 (2020) 108134.
[29] J. Avsec, Int. J. Heat Mass Transf. 51 (2008) 4589–4598.
[30] G. Chen, Int. J. Therm. Sci. 39 (2000) 471–480.
[31] G.L. Pollack, Rev. Mod. Phys. 41 (1969) 48.
[32] C. Huang, X. Qian, R. Yang, Mater. Sci. Eng. R-Rep. 132 (2018) 1–22.
[33] S.U. Ilyas, R. Pendyala, M. Narahari, Colloid. Surface. A 527 (2017) 11–22.
[34] K. Wang, J. Pang, L. Li, S. Zhou, Y. Li, T. Zhang, Front. Chem. Sci. Eng. 12 (2018) 376–382.
[35] B. Bakthavatchalam, K. Habib, R. Saidur, S. Shahabuddin, B.B. Saha, Nanotechnology 31 (2020) 235402.
[36] T. Aziz, H. Fan, F.U. Khan, M. Haroon, L. Cheng, Polym. Bull. 76 (2019) 2129–2145.
[37] Z. Wu, M. Qin, M. Zhang, Energ. Build. 174 (2018) 254–261.
[38] L. Hospers, J.W. Smallcombe, N.B. Morris, A. Capon, O. Jay, Sci. Total Environ. 747 (2020) 141180.
[39] J.W. Lee, S. Kim, I.T. Pineda, Y.T. Kang, Renew. Sust. Energ. Rev. 138 (2021) 110524.
[40] V. Linek, M. Kordač, M. Soni, Chem. Eng. Sci. 63 (2008) 5120–5128.
[41] J.H.J. Kluytmans, B.G.M. van Wachem, B.F.M. Kuster, J.C. Schouten, Chem. Eng. Sci. 58 (2003) 4719–4728.
[42] G. Liang, I. Mudawar, Int. J. Heat Mass Transf. 146 (2020) 118864.
[43] Z. Li, B. Cheng, J. Ju, W. Kang, Y. Liu, Desalination 501 (2021) 114834.
[44] S. He, G. Chen, H. Xiao, G. Shi, C. Ruan, Y. Ma, H. Dai, B. Yuan, X. Chen, X. Yang, J. Colloid. Interf. Sci. 582 (2021) 90–101.
[45] Y. Zhou, T. Yan, W. Pan, Int. J. Energ. Res. 45 (2021) 9719–9752.
[46] A. Golkhar, P. Keshavarz, D. Mowla, J. Membr. Sci. 433 (2013) 17–24.
[47] M. Rezakazemi, M. Darabi, E. Soroush, M. Mesbah, Sep. Purif. Technol. 210 (2019) 920–926.

[48] L. Jorge, S. Coulombe, P.L. Girard-Lauriault, Plasma Process. Polym. 12 (2015) 1311–1321.
[49] Y. Cao, Z.U. Rehman, N. Ghasem, M. Al-Marzouqi, N. Abdullatif, A.T. Nakhjiri, M. Ghadiri, M. Rezakazemi, A. Marjani, M. Pishnamazi, S. Shirazian, Sci. Rep. 11 (2021) 1–12.
[50] I.C. Gerber, P. Serp, Chem. Rev. 120 (2020) 1250–1349.
[51] S. Li, Z. Fan, Energy Storage Mater. 34 (2021) 107–127.
[52] J.H. Lee, J.W. Lee, Y.T. Kang, Appl. Therm. Eng. 103 (2016) 980–988.
[53] L.W. Fan, J.Q. Li, Y.Z. Wu, L. Zhang, Z.T. Yu, Appl. Therm. Eng. 122 (2017) 555–565.
[54] R. Das, M.E. Ali, S.B. Abd Hamid, S. Ramakrishna, Z.Z. Chowdhury, Desalination 336 (2014) 97–109.
[55] S. Velioglu, H.E. Karahan, K. Goh, T.H. Bae, Y. Chen, J.W. Chew, Small 16 (2020) 1907575.
[56] Korea Meteorological Admistration, Weather Information (Seoul, South Korea 2020), https://www.weather.go.kr, Accessed January 23, 2021.
[57] B. Zhao, F. Liu, Z. Cui, C. Liu, H. Yue, S. Tang, Y. Liu, H. Lu, B. Liang, Appl. Energ. 185 (2017) 362–375.
[58] S.Y. Oh, M. Binns, H. Cho, J.K. Kim, Appl. Energ. 169 (2016) 353–362.
[59] M.N.A.W.M. Yazid, N.A.C. Sidik, W.J. Yahya, Renew. Sust. Energy Rev. 80 (2017) 914–941.
[60] Z. Duan, R. Sun, Chem. Geol. 193 (2003) 257–271.
[61] Y.H. Chen, D.L. Lu, Appl. Clay Sci. 104 (2015) 221–228.
[62] F. Su, C. Lu, Energ Environ. Sci. 5 (2012) 9021–9027.
[63] F. Jiang, S. Hu, Y.-L. Hsieh, ACS Appl. Nano Mater. 1 (2018) 6701–6710.
[64] J. Ouyang, W. Gu, C. Zheng, H. Yang, X. Zhang, Y. Jin, J. Chen, J. Jiang, Appl. Clay Sci. 152 (2018) 267–275.
[65] Q. Guo, C. Chen, Z. Li, X. Li, H. Wang, N. Feng, H. Wan, G. Guan, Chem. Eng. J. 371 (2019) 414–423.
[66] K. Huang, L. Liang, S. Chai, U. Tumuluri, M. Li, Z. Wu, B.G. Sumpter, S. Dai, J. Mater. Chem. A 5 (2017) 16241–16248.
[67] Y. Guo, C. Tan, J. Sun, W. Li, J. Zhang, C. Zhao, Fuel 259 (2020) 116298.
[68] C. Yang, D. Liu, Y. Chen, C. Chen, J. Wang, Y. Fan, S. Huang, W. Lei, ACS Appl. Mater. Inter. 11 (2019) 10276–10282.
[69] C.F. Cogswell, H. Jiang, J. Ramberger, D. Accetta, R.J. Willey, S. Choi, Langmuir 31 (2015) 4534–4541.
[70] A.U. Maheswari, K. Palanivelu, J. CO2 Util. 6 (2014) 45–52.
[71] A.U. Maheswari, K. Palanivelu, Environ. Sci. Pollut. Res. 24 (2017) 5733–5745.
[72] H.M. Mohsin, A.M. Shariff, K. Johari, Sep. Purif. Technol. 222 (2019) 297–308.
[73] H.M. Mohsin, K. Johari, A.M. Shariff, Fuel 232 (2018) 454–462.
[74] S. Kim, R. Xu, H.S. Lim, Y.T. Kang, Adv. Mater. Interfaces 7 (2020) 2000618.